Integration of LTE and GNSS Antenna for Multiband Performance in Vehicular Application

Amruta A. Nikam* and Rupali B. Patil

Abstract—The paper proposes a antenna design that can serve as a comprehensive solution for covering 4G/5G cellular bands 850–1000 MHz, 1900 MHz, 2100–2700 MHz, 3300–4900 MHz, Global Navigation Satellite System (GNSS-L1) Band 1.56 GHz–1.61 GHz, V2X 5.850–5.925 GHz band which are appropriate for the use in automobile applications. The proposed antenna is designed with respective polarization for cellular and GNSS applications, where the cellular antenna is linearly polarized, and the GNSS antenna is circularly polarized by chamfering the square patch. FR4 substrate material is used to construct the Long Term Evolution/4G (LTE) antenna. The optimization of the antennas ensures minimal coupling between them. The cellular antenna is designed using a hexagonal base with a modified ground plane to achieve the required cellular bands using a monopole (fractal design). The GNSS antenna is implemented on a PVC (Poly Vinyl Chloride) substrate. The measured results of S_{11} parameter show that the proposed design covers all the required 4G/5G bands with minimum S_{11} of -10 dB and a radiation pattern in the theta 60–90° range for cellular antenna, while the GNSS antenna has a zenith radiation pattern with axial ratio of < 3 dB for theta angles in the 0–30° range and a mutual coupling of -15 dB. The fabricated antenna was measured to validate the simulated results of reflection coefficient. All things considered, the suggested design is perfect for automobile applications to satisfy both satellite and mobile communication needs.

1. INTRODUCTION

Recent advancements in autonomous driving and intelligent vehicles have led to a significant increase in research and development of vehicular communication systems and protocols. As a result, vehicle-to-everything (V2X) technology has been developed, including communications among vehicles, pedestrians, infrastructure, and networks. V2X can boost security, effectiveness, and traffic flow in the transportation system by facilitating communication between cars, infrastructure, and pedestrians [1]. In order to meet the requirement of vehicle communication (V2X), 5G sub-6 GHz, wireless technology plays a crucial role in enabling V2X communication and supporting various applications such as accelerative collision threatening, vehicle parking space, and traffic optimization [2]. The Global Navigation Satellite System (GNSS) plays a vital role in V2X communication. However, on its own, GNSS may not provide the desired level of accuracy. To overcome this limitation, GNSS is often combined with other system [3]. The focus of this study is to propose an integration of LTE monopole and GNSS antennas that can cover the 5G sub-6 GHz, V2X, and GNSS frequency bands. Prior research had mostly concentrated on only LTE frequency ranges between 698 MHz and 2690 MHz [4–13]. Monopoles and planar inverted-F type of antennas (PIFAs) are the most widely utilized LTE antenna types. However, there are a limited number of LTE monopole antennas reported in the literature that

can effectively cover the 5G sub-6 GHz frequency band [14–16]. These monopole antennas only occupy 5G sub-6 GHz frequencies and do not cover other bands.

Antennas based on metamaterial and metasurfaces using ultra-wideband (UWB) technology are promising candidates for the 5G sub-6 GHz frequency range [17–20]. However, previous research has shown that certain designs, such as the PIFA, may not be suitable for smaller shark-fins due to their large size [21]. While UWB antennas have been developed for 5G sub-6 GHz and V2X bands, they may not be suitable for the use inside a shark-fin [22]. The shark-fin case of vehicle roof top has been filled with several antennas, which can enhance mutual coupling among various antennas. Hence, researchers are designing antennas that cover various bands and use cases to counteract these impacts, using fewer antennas. By using multi-band antennas, the quantity of antennas inside the shark fin can be minimized, reducing shadowing and coupling effects and improving overall antenna performance [23]. In general, vehicle has separate antennas for cellular communication (LTE antenna) and navigation (GNSS antenna) because the two types of antennas show different polarization performances. A very few antennas are reported in literature which combine cellular antenna and navigation antenna [24, 25].

In light of the literature survey presented, it is evident that compressed multiband antennas are essential for vehicular use. The present study reports a multiband antenna, but very few researches have been done on integration of GNSS/5G/V2X frequency band. To achieve this, there is a need to integrate antennas into a single solution, which could potentially address the challenges of limited space and antenna performance in a vehicular setting.

In this work, a multiband monopole antenna is proposed to cover 5G sub-6 GHz, V2X and GNSS frequencies. The planned antenna is a 3-D LTE antenna that features fractal geometry, allowing it to cover a frequency ranging 850 MHz–5.9 GHz. The LTE monopole antenna covers 5G sub-6 GHz and V2X band, and horizontal patch antenna covers GNSS frequency band. The primary objective of this research is to develop a multiband antenna specifically tailored for vehicle communication. The study focuses on enhancing the antenna's performance in terms of multiband capability, mutual coupling reduction, and polarization characteristics. Various techniques are employed throughout the research, including the utilization of a unique antenna design, simulation using the High Frequency Structured Simulator (HFSS), and fabrication of the antenna. The design process incorporates these techniques to achieve the desired outcomes and optimize the antenna's performance for vehicle communication applications. It is important to note that an LTE vertical antenna is a linearly polarized antenna, and a GNSS horizontal antenna is an right hand circular polarization (RHCP) one. The proposed antenna in this study is designed to accommodate both polarizations. The design procedure of the antenna is presented in Section 2, while Section 3 deliberates the results of the antenna. Finally, Section 4 concludes the study.

2. GEOMETRY OF ANTENNA DESIGN PROPOSED

The antenna design process involved separate designs of a vertical LTE antenna and a horizontal GNSS antenna. Each antenna was simulated individually. After designing the separate antennas, they were integrated, and the mutual coupling between them was examined. The LTE antenna has dimensions of $68 \times 35 \times 1.6$ mm^3 and is composed of hexagonal elements with a side length of 3 mm as shown in Figure 2. The feed pad of the LTE antenna has dimensions of 5.5×3.5 mm^2. The GNSS antenna has dimensions of $54 \times 54 \times 6.8$ mm^3, and its feed position is located 19 mm away from the centre of the model. The simulation process is sequential, where one port is simulated at a time, and the other port is considered to be 50 Ohm. The LTE antenna is fabricated using an FR4 substrate as GNSS antenna fabricated using polyvinyl chloride (PVC) material.

2.1. The Antenna Design for GNSS Antenna

The length and width of the rectangular patch are calculated from the standard expressions available in the literature [26]. The GNSS L1 band (1.56–1.61 GHz) antenna was designed with a specific frequency of operation at 1.585 GHz. For the antenna's substrate material, a PVC material with a thickness of 6.8 mm was utilized. According to the formulae [26] the length and width of the patch come to be 84.85 and 95.23 mm, respectively. But in order to keep the patch a square, to get better circular field

rotation, simply keep $W = L$, which makes the antenna resonate at lower frequency. Then to achieve exact frequency of 1.575 GHz, it was needed to reduce L to 54 mm, as reduction in patch dimensions increases the operating frequency. The chamfering of the edges was done on trial and error basis, to get the best axial ratio. The rectangular cut in the GNSS center was made to accommodate the LTE structure. The rectangular slot has a width of 19 mm and a length of 30 mm. The patch corners are chamfered to create circular polarization (CP) radiation. The ground plane measures 54 mm $\times$ 54 mm; the patch radiator is 49.6 mm $\times$ 49.6 mm; the substrate is 6.8 mm thick; and the coaxial feed probe has a 1.4 mm diameter. The dimension of GNSS antenna is depicted in Figure 1. Further the dimensions of the cut were optimized to achieve minimum S_{21} between the antennas in common frequency of GNSS band. The best possible mutual coupling is -15 dB decoupling.
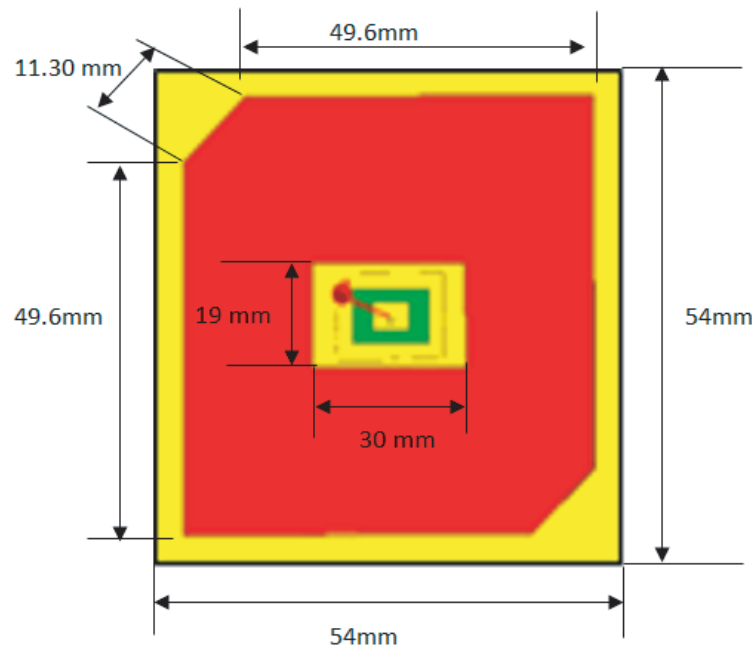
Figure 1. Layout of GNSS antenna.

2.2. The Antenna Design for LTE Antenna

FR4 substrate material of thickness 1.6 mm is used to create the LTE antenna with loss tangent of 0.02. To cover a frequency band ranging from 850 MHz to 1000 MHz, 1900 MHz, 2100 MHz to 2700 MHz, and 3300 MHz to 6000 MHz, a hexagonal fractal shape was used to design the LTE antenna. The LTE antenna has dimensions of $35 \times 68 \times 1.6$ mm^3 and is composed of hexagonal elements with a side length of 3 mm. The feed pad for the LTE antenna measures 5.5×3.5 mm^2. The hexagonal shape was chosen due to its ability to achieve multiple bands, and many fractal antennas are designed using this shape with multiple iterations to further reduce return losses [27]. The proposed antenna design has undergone several iterations, including both basic and fractal iterations, as illustrated in Figure 3.

The LTE antenna design divided into three parts, long arm, short arm, and lower parts of antenna. To cover the LTE frequency bands, a monopole antenna was used, where a long arm was incorporated to cover the 800–900 MHz band, followed by a smaller and wider arm to cover the 1.7–2.7 GHz band. The higher 3–6 GHz bands were achieved through the lower part of the antenna, using simple $\lambda/4$ calculations. To give the antenna multiple frequency band characteristics, fractal iterations were utilized using hexagonal shape. The dimension of hexagonal shape is shown in Figure 2. The iterations are performed till the achievement of multiband frequencies. In achieving the intended operating frequency characteristics of the antenna, the ground plane is a crucial component. The proposed design contains a defective ground structure [28–30] in its partial ground plane, as seen in Figure 4.
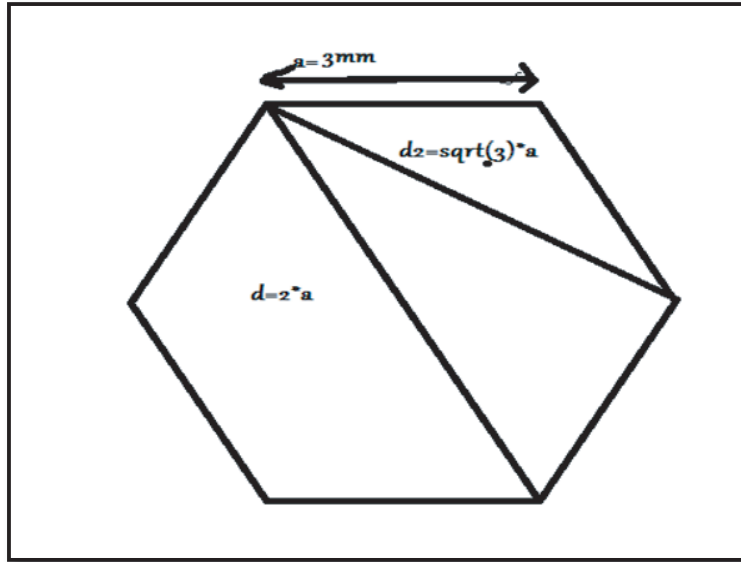
Figure 2. The figure illustrates the dimensions of the hexagonal shape used in the antenna design, where $d = 2 \times a$, $d_2 = sqrt(3) \times a$, $p = 6 \times a$, Height $= d_2 = 2 \times ri$.
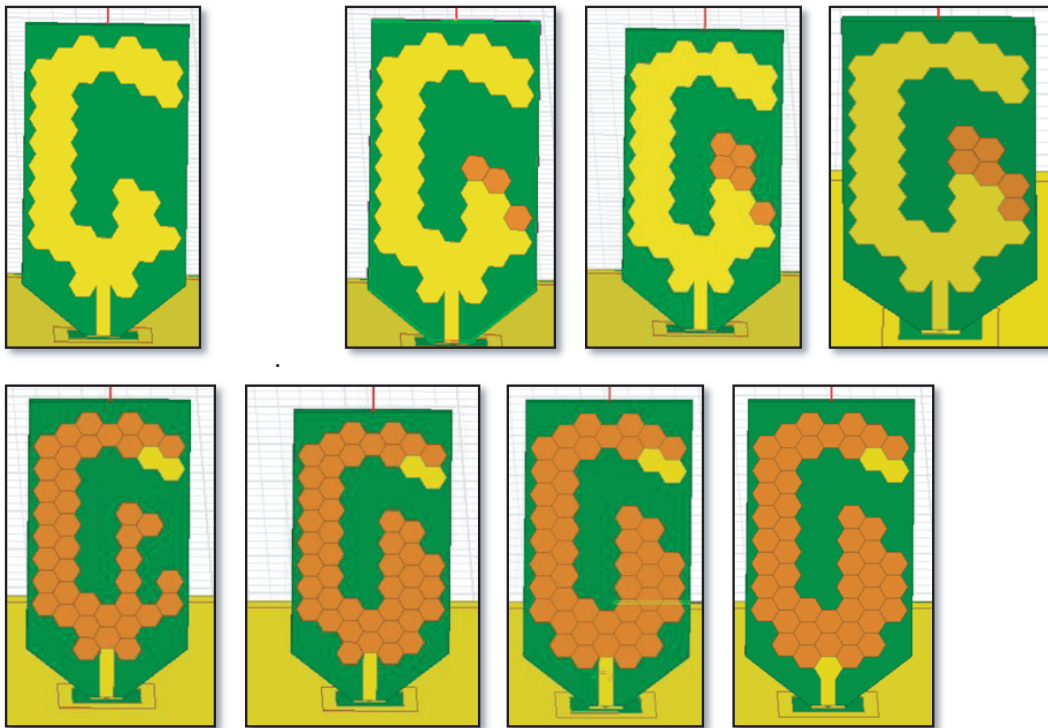
Figure 3. Design steps of LTE Antenna structure.

The formula to calculate the length (L) of a monopole antenna assumes that it is a quarter-wavelength $(\lambda/4)$ monopole and operating in free space. Calculations were made to determine the length of the monopole antenna, which was designed to operate at a quarter-wavelength $(\lambda/4)$. The equation expresses the effective wavelength (λ_{eff}) of an electromagnetic wave traveling through a material with relative permittivity (ε_r) and height-to-width ratio (h/w). The effective permittivity (ε_{reff}) is calculated
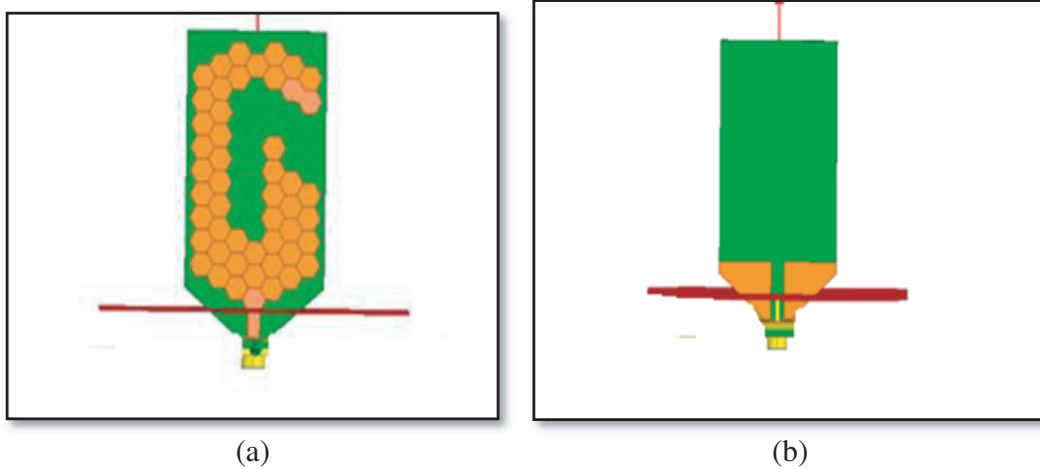
Figure 4. Proposed geometry of integration of LTE and GNSS antenna. (a) Front view of LTE antenna. (b) Back view of LTE antenna.

based on the relative permittivity and height-to-width ratio. The effective wavelength is calculated using the frequency of the wave and the effective permittivity (ε_{reff}). The detailed dimension of the LTE antenna is shown in Table 1.

$$\lambda_{eff} = e^x = \frac{3*10^{11}}{Freq*10^6*sqrt(\varepsilon_{reff})}, \quad \varepsilon_{reff} = 1 + \frac{\varepsilon_r + 1}{2} + \frac{\varepsilon_r - 1}{2}\left(1 + \frac{12h}{w}\right)^{-1/2} \tag{1}$$

where λ_{eff}: effective wavelength, ε_r: relative permittivity, (ε_{reff}): effective permittivity, effective permittivity (ε_{reff}).

To improve the use of a vehicular antenna, several techniques can be employed, including Fractal Geometry to achieve multiband operation, Defected Ground Structure for bandwidth (BW) enhancement, Chamfering the edges of the patch for circular polarization and to achieve a desirable axial bandwidth ratio. A prototype for the proposed antenna is fabricated as shown in Figure 5.
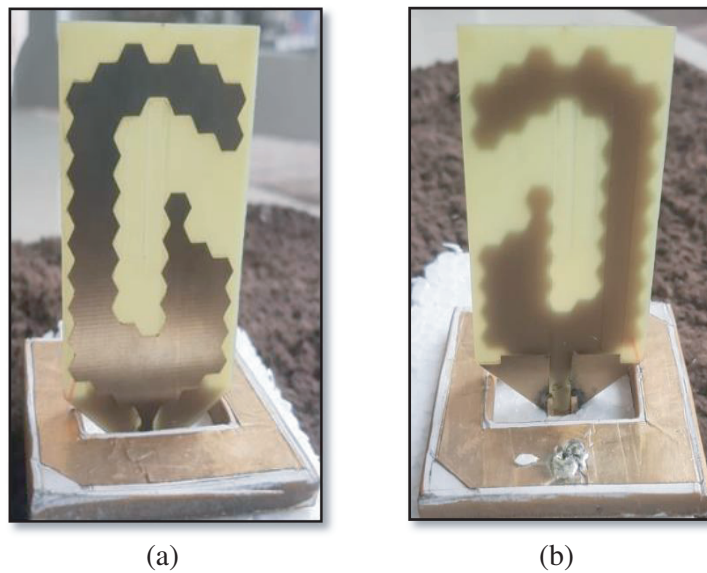
Figure 5. Proposed fabricated antenna. (a) Front view of LTE antenna. (b) Back view of LTE antenna.

Table 1. Detailed dimensions of the LTE antenna.

Frequency	λ(mm)	λ/4(mm)	Λeffective(mm)	Λeffective/4(mm)
800	375	93.75	176.78	44.19
900	333.33	83.33	157.13	39.28
1700	176.47	44.12	83.19	20.80
2300	130.43	32.61	61.49	15.37
2700	111.11	27.78	52.38	13.09
3300	90.91	22.73	42.85	10.71
3900	76.92	19.23	36.26	9.07
4500	66.67	16.67	31.43	7.86
5000	60.00	15.00	28.28	7.07

3. SIMULATION OF PROPOSED DESIGN AND RESULT DISCUSSION

To measure GNSS antenna, only port 1 is stimulated while the other ports are terminated with a 50-Ω load. The same approach is followed for measuring the LTE antenna where the corresponding port is stimulated, and a 50-Ω load is connected to the remaining ports. The objective of this section is to discuss the parameters used in vehicular communication, with a primary focus on the return loss (S_{11} parameter). This parameter is crucial as it indicates the percentage of the signal traveling in the forward direction. According to [31], a minimum return loss of -15 dB is crucial for real-time vehicular communications, while [32] suggests that the standing wave ratio should be within the range of 1 dB to 3 dB for vehicular communications.

   The return losses of the GNSS and LTE antennas at their respective frequencies were analysed, and the results are shown in Figure 6 and Figure 7.

   The analysis reveals that the GNSS antenna has better return loss performance, indicating that it performs well within the desired frequency band. Specifically, the GNSS antenna has a return loss of
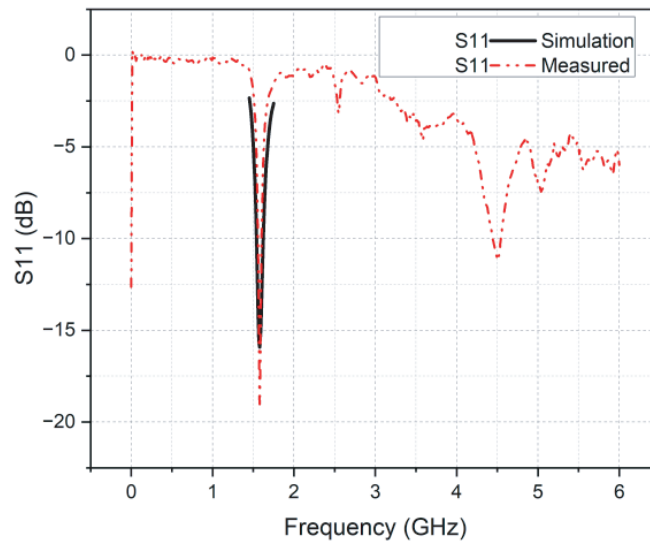
Figure 6. Simulated and measured S_{11} parameter of GNSS antenna.
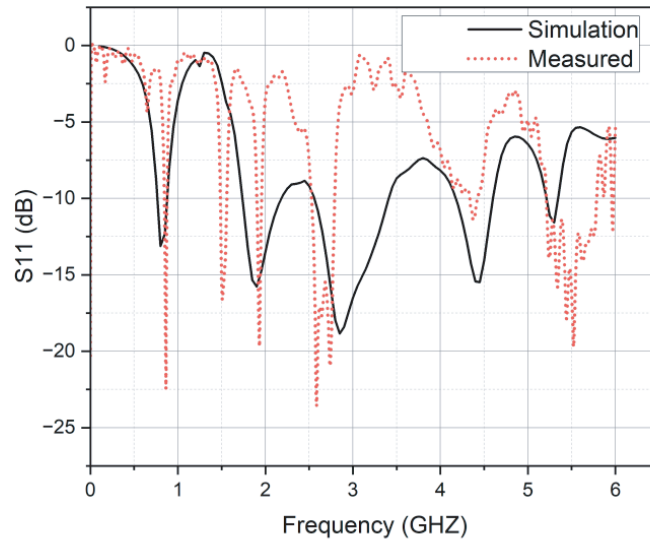
Figure 7. Simulated and measured S_{11} parameter of LTE antenna.

-19.07 dB at 1.57 GHz, and this result was obtained by cutting a square patch antenna at its centre. Cutting the antenna at its centre creates two smaller radiating patches, which swings the resonant frequency of the antenna to a higher frequency due to the reduced surface area and smaller wavelength.

The simulated return loss results for the LTE antenna reveal a return loss of -13.13 dB at 864 MHz, -15.77 dB at 1.9 GHz, -18.84 dB at 2.85 GHz, -15.42 dB at 4.4 GHz, -11.42 dB at 5.2 GHz, and -8.84 dB at 5.86 GHz. On the other hand, the measured return loss results indicate a return loss of -22.45 dB at 864 MHz, -19.69 dB at 1.93 GHz, -22.77 dB at 2.5 GHz, -10.94 dB at 4.4 GHz, -19.24 dB at 5.5 GHz, and -9.97 dB at 5.86 GHz. The LTE antenna performs optimally across different frequency bands, including 846–876 MHz, 1.75–2.2 GHz, 2.5–3.5 GHz, 4.15–4.6 GHz, 5.2–5.7 GHz, and 5.7–5.98 GHz as shown in Figure 7.

To accommodate the LTE PCB, a cut of 30 mm × 19 mm was made in the GNSS centre, and to improve isolation its dimensions were optimized to minimize S_{21} between the antennas at the GNSS band's common frequency. The approach used here leads to a low level of coupling between the resonances of the GNSS antenna and LTE antenna. As a result, the antenna design is capable of operating effectively across various frequency bands. The optimal performance achieved through this optimization is a decoupling up to -15 dB as shown in Figure 8.

The bottom square patch of the GNSS antenna is sliced into two opposed corners as part of the suggested antenna design in order to excite two orthogonal modes and achieve circular polarization. The truncated square patch has a square-shaped groove etched into it to increase the impedance bandwidth and axial ratio (AR) bandwidth of the antenna in the low band, and a coaxial probe is utilized for impedance matching. However, having a thicker PVC substrate might enhance bandwidth while also increasing the inductance caused by the feeding probe, which makes impedance matching more difficult. In order to better match impedance, a square-shaped slot is added to create a capacitance that suppresses the inductance the probe causes. The AR of 1.19 dB with AR BW 65 MHz is shown in Figure 9.

In the GNSS frequency band, the simulated gain achieved is around 8.25 dBi, indicating a high level of signal amplification for satellite communication. In the LTE high band, which refers to the higher frequencies of the LTE spectrum, the gain varies from 1 dBi to 7.25 dBi. In the LTE middle band, which refers to the middle range of the LTE spectrum, the gain varies from 2.4 dBi to 5.6 dBi. However, in the lower frequency band, the gain is less than -1 dBi, which means that the antenna does not amplify signals within this range. Overall, the proposed antenna design is capable of providing high gain across multiple frequency bands, making it suitable for a wide range of communication applications. The 3-D radiation pattern of antenna is shown in Figure 10.
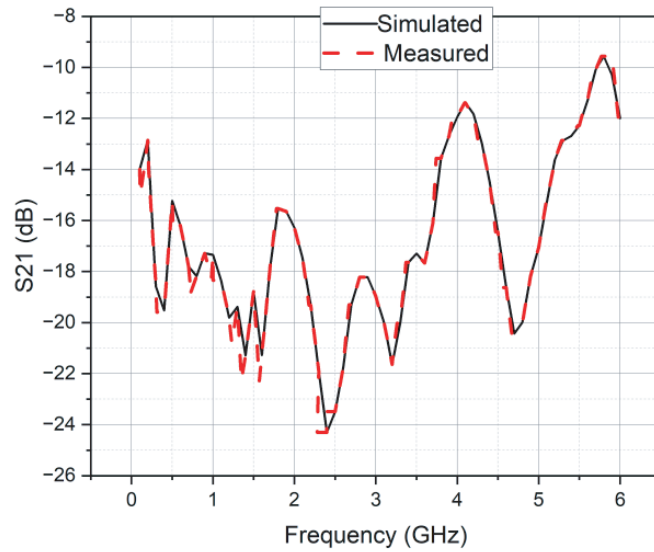
Figure 8. Simulated and measured S_{21} parameter (mutual coupling) of proposed antenna.

Table 2 provides a summary of the judgment between the performance of the proposed multiband antenna design and that of previously reported multiband antennas for various frequency ranges and applications.

Table 2. Comparison between proposed antenna and existing multiband antenna.

Ref	Size(mm3)	Material	Operating Frequency(GHz)	Feeding Method	Bandwidth/Axial ratio BW (%,HZ)	Return Loss(S11 Parameter)	Gain(dbi)	Application
[33]	175× 47 × 1.7	FR4	1.75,1.85,1.95,2.15,2.6	Co-axial Feed	NA	S11<-10dB	2.1,-1.7,1.9,3.2,4.8	LTE,WLAN
[34]	58×40×1.6	FR4	1.51-3.69/4.67-5.25/5.78-5.96	Co-axial Feed	83.8/11.69/3.06	S11<-10dB	5.2/4.8/5	vehicle-to-vehicle communication
[35]	70 * 30 *1.6	FR4	770 MHz–1000 MHz / 1.7 GHz–3.78 GHz	Co-axial Feed	240MHZ/2400MHZ	S11<-10dB	3.54/5.89/3.52	GSM, LTE, and 5G.
[36]	51 * 52 * 1.6	FR4	1.17645 GHz/2.320–2.345 GHz/1.9GHz	Co-axial Feed	ARBW=12MHZ/25MHZ	S11<-10dB	3/6.5	GPS L5,SDARS,GSM-1900
[37]	87.5 × 61 × 1.6 mm	FR4	1.8–2.9, 3.4–4.6, and 5–5.6	Co-axial Feed	NA	S11<-10dB	2.58–3.34dbi	WLAN
This Work	68x54x1.6	FR4 & PVC	1.57-1.61GHz,846-876 MHz, 1.75-2.2 GHz, 2.5-3.5 GHz, 4.15-4.6 GHz, 5.2-5.7 GHz, and 5.7-5.98 GHz.	Co-axial Feed	ARBW for GNSS= 65 MHz,LTE 10dB BW: 800-910 MHz 1740-3500 MHz 4250-4650 MHz 5150-5400 MHz	S11<-10dB	8.25dbi at 1.57GHz,LTE from 1dbi to 8.12dbi,V2X - 4.65dbi	GNSS,LTE,V2X
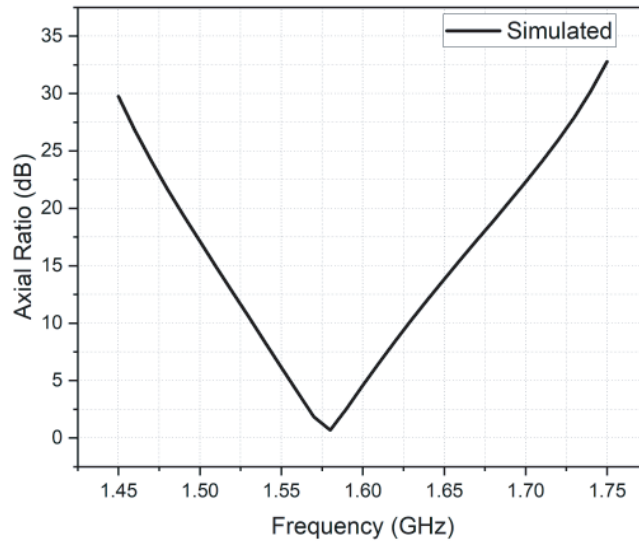
Figure 9. Simulated axial ratio of GNSS antenna.

(a)

(b)

(c)

(d)

(e)

(f)

(g)

(h)

(i)
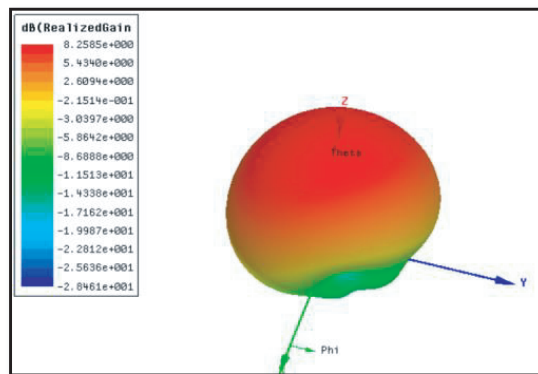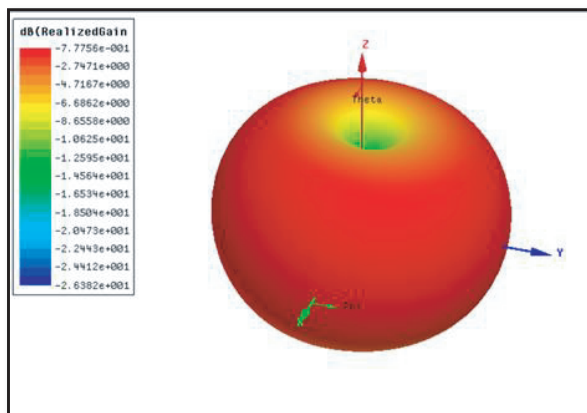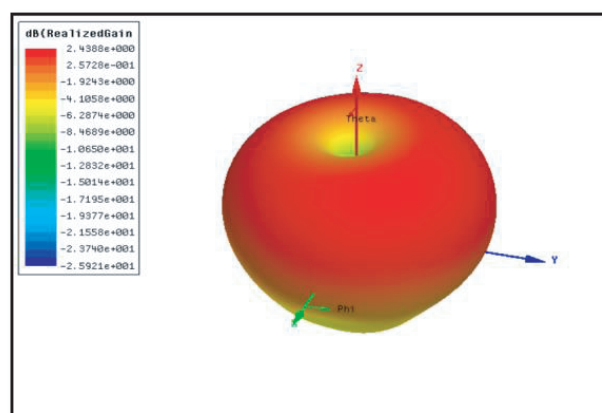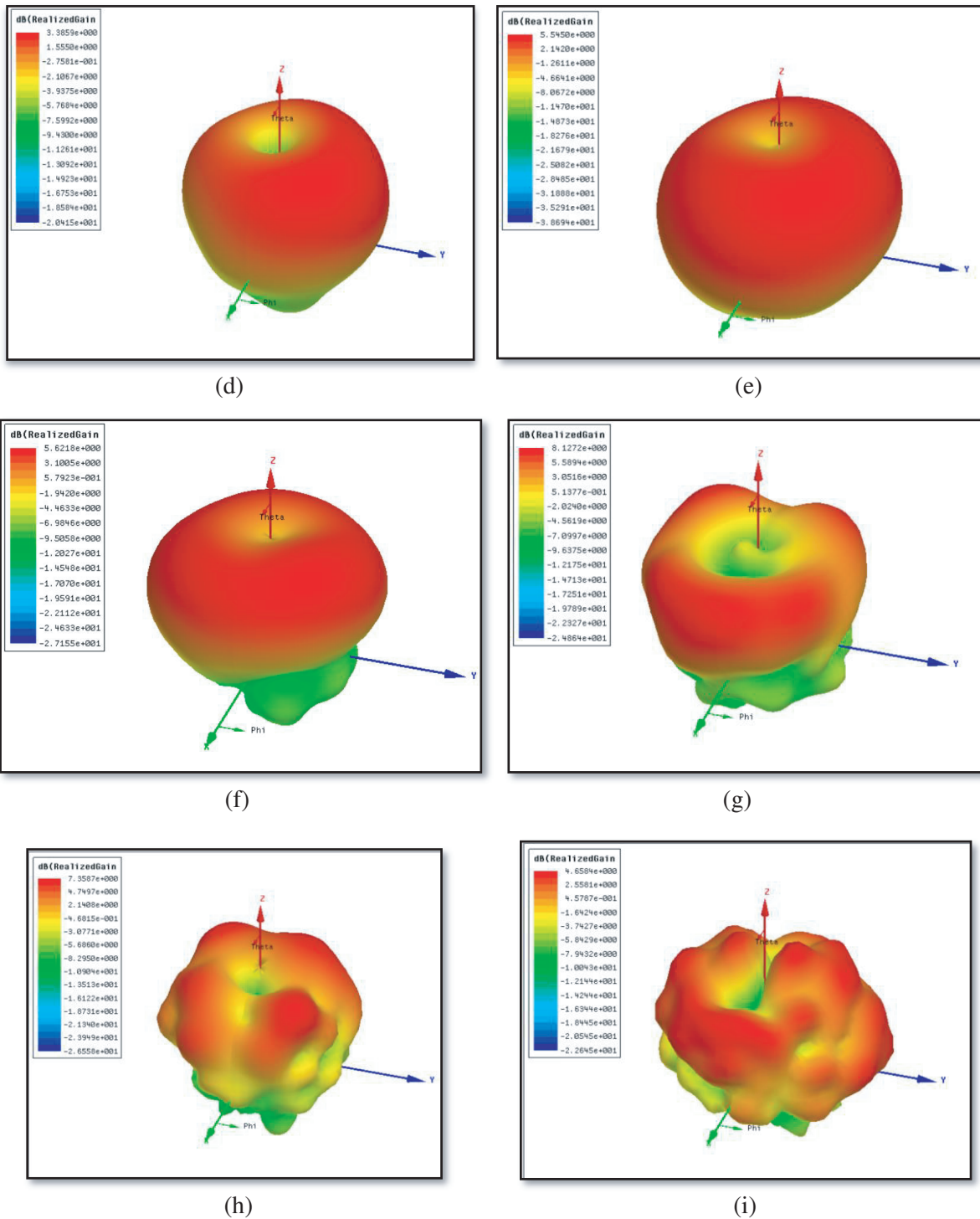
Figure 10. Radiation pattern (realized) at different frequencies. (a) Realized gain (dBic) — GNSS at 1.575 GHz. (b) Realized gain (dBic) — LTE frequency = 0.85 GHz. (c) Realized gain (dBic) — LTE frequency = 1.71 GHz. (d) Realized gain (dBic) — LTE frequency = 2.1 GHz. (e) Realized gain (dBic) — LTE frequency = 2.7 GHz. (f) Realized gain (dBic) — LTE frequency = 3.5 GHz. (g) Realized gain (dBic) — LTE frequency = 4.4 GHz. (h) Realized gain (dBic) — LTE frequency = 5.3 GHz. (i) Realized gain (dBic) — LTE frequency = 5.85 GHz.

4. CONCLUSION

The paper proposes a multiband antenna design with different polarizations, allowing it to operate across multiple frequency bands and transmit signals in various orientations. The performance of the antenna was validated by fabricating and testing a fully functional prototype. Both simulation and measurement results demonstrated the antenna's efficacy across different frequency ranges, indicating its potential for the use in various communication applications. Additionally, simulation results revealed that the proposed antenna design had a high gain, which is a measure of signal amplification. Based on these features and performance, the paper concludes that the proposed antenna is suitable for vehicular communications.

REFERENCES

1. Alibakhshikenari, M., B. S. Virdee, C. H. See, et al., "Dual-polarized highly folded bowtie antenna with slotted self-grounded structure for sub-6 GHz 5G applications," *IEEE Transactions on Antennas and Propagation*, Vol. 70, No. 4, 3028–3033, 2021.

2. Gyawali, S., S. Xu, Y. Qian, and R. Q. Hu, "Challenges and solutions for cellular based V2X communications," *IEEE Communications Surveys & Tutorials*, Vol. 23, No. 1, 222–255, 2021.

3. Wen, W. W., G. Zhang, and L.-T. Hsu, "GNSS NLOS exclusion based on dynamic object detection using LiDAR point cloud," *IEEE Transactions on Intelligent Transportation Systems*, Vol. 22, No. 2, 853–862, Feb. 2021.

4. Preradov, D. and D. N. Aloi, "Cross polarized 2 × 2 LTE MIMO system for automotive shark fin application," *Applied Computational Electromagnetics Society*, Vol. 35, No. 10, 1207–1216, 2020.

5. Dong, Y., J. Choi, and T. Itoh, "Vivaldi antenna with pattern diversity for 0.7 to 2.7 GHz cellular band applications," *IEEE Antennas and Wireless Propagation Letters*, Vol. 17, No. 2, 247–250, Feb. 2018.

6. Arianos, S., G. Dassano, F. Vipiana, and M. Orefice, "Design of multi-frequency compact antennas for automotive communications," *IEEE Transactions on Antennas and Propagation*, Vol. 60, No. 12, 5604–5612, 2012.

7. Michel, A., P. Nepa, M. Gallo, I. Moro, A. P. Filisan, and D. Zamberlan, "Printed wideband antenna for LTE-band automotive applications," *IEEE Antennas and Wireless Propagation Letters*, Vol. 16, 1245–1248, 2017.

8. Liu, Y., Z. Ai, G. Liu, and Y. Jia, "An integrated shark-fin antenna for MIMO-LTE, FM, and GPS applications," *IEEE Antennas and Wireless Propagation Letters*, Vol. 18, No. 8, 1666–1670, Aug. 2019.

9. Franchina, V., A. Michel, P. Nepa, M. Gallo, and R. Parolari, "A compact 3D antenna for automotive LTE MIMO applications," *Proceedings of the 2017 IEEE-APS Topical Conference on Antennas and Propagation in Wireless Communications, APWC*, 326–329, Verona Italy, Sept. 2017.

10. Friedrich, A., B. Geck, O. Klemp, and H. Kellermann, "On the design of a 3D LTE antenna for automotive applications based on MID technology," *Proceedings of the 2013 European Microwave Conference*, 640–643, Nuremberg, Germany, Oct. 2013.

11. Goncharova, I. and S. Lindenmeier, "A high efficient automotive roof-antenna concept for LTE, DAB-L, GNSS and SDARS with low mutual coupling," *Proceedings of the 2015 9th European Conference on Antennas and Propagation, EuCAP*, 1–5, Lisbon, Portugal, Apr. 2015.

12. Goncharova, I. and S. Lindenmeier, "A high-efficient 3-D Nefer-antenna for LTE communication on a car," *Proceedings of the 8th European Conference on Antennas and Propagation, EuCAP*, 3273–3277, e Hague, Netherlands, Apr. 2014.

13. Navarro-Mendez, D. V., L. F. Carrera-Suarez, E. Antoninó-Daviu, et al., "Compact wideband Vivaldi monopole for LTE mobile communications," *IEEE Antennas and Wireless Propagation Letters*, Vol. 14, 1068–1071, 2015.

14. Yacoub, A. M., M. O. Khalifa, and D. N. Aloi, "Design of multi-wideband Automotive cell antenna for LTE and 5G applications," *2021 15th European Conference on Antennas and Propagation, EuCAP*, 2021.

15. Sanz-Izquierdo, B., S. Jun, J. Heirons, and N. Acharya, "Inkjet printed and folded LTE antenna for vehicular application," *Proceedings of the 2016 46th European Microwave Conference (EuMC)*, 88–91, London, UK, Oct. 2016.

16. Cheng, Y., J. Lu, and C. Wang, "Design of a multiple band vehicle-mounted antenna," *International Journal of Antennas and Propagation*, Vol. 2019, Article ID 6098014, 11 pages, 2019.

17. Sadeghzadeh, R. A., M. Alibakhshi-Kenari, and M. Naser Moghadasi, "UWB antenna based on SCRLH-TLs for portable wireless devices," *Microwave and Optical Technology Letters*, Vol. 58, No. 1, 69–71, 2016.

18. Alibakhshi-Kenari, M., M. Naser-Moghadasi, R. Ali Sadeghzadeh, and B. Singh Virdee, "Metamaterial-based antennas for integration in UWB transceivers and portable microwave handsets," *International Journal of RF and Microwave Computer-Aided Engineering*, Vol. 26, No. 1, 88–96, 2016.

19. Alibakhshi-Kenari, M., M. Naser-Moghadasi, R. Ali Sadeghzadeh, B. Singh Virdee, and E. Limiti, "New compact antenna based on simplified CRLH-TL for UWB wireless communication systems," *International Journal of RF and Microwave Computer-Aided Engineering*, Vol. 26, No. 3, 217–225, 2016.

20. Alibakhshikenari, M., B. S. Virdee, A. Ali, and E. Limiti, "Extended aperture miniature antenna based on CRLH metamaterials for wireless communication systems operating over UHF to C-band," *Radio Science*, Vol. 53, No. 2, 154–165, Feb. 2018.

21. Yacoub, A., M. Khalifa, and D. N. Aloi, "Wide bandwidth low profile PIFA antenna for vehicular sub-6 GHz 5G and V2X wireless systems," *Progress In Electromagnetics Research C*, Vol. 109, 257–273, 2021.

22. Hasturkoglu, S. and S. Lindenmeier, "A wideband automotive antenna for actual and future mobile communication 5G/LTE/WLAN with low profile," *Proceedings of the 2017 11th European Conference on Antennas and Propagation, EUCAP*, 602–605, Paris, France, Mar. 2017.

23. Artner, G., W. Kotterman, G. Del Galdo, and M. A. Hein, "Automotive antenna roof for cooperative connected driving," *IEEE Access*, Vol. 7, 20083–20090, 2019.

24. Ge, L., S. Gao, Y. Li, W. Qin, and J. Wang, "A low-profile dual-band antenna with different polarization and radiation properties over two bands for vehicular communications," *IEEE Transactions on Vehicular Technology*, Vol. 68, No. 1, 1004–1008, 2019.

25. Sharma, Y., D. Sarkar, K. Saurav, and K. V. Srivastava, "Three-element MIMO antenna system with pattern and polarization diversity for WLAN applications," *IEEE Antennas and Wireless Propagation Letters*, Vol. 16, 1163–1166, 2016.

26. Balanis, C. A., *Microstrip Antennas, Antenna Theory, Analysis and Design*, 3rd Edition, John Wiley & Sons, 2010.

27. Rahim, A. and P. K. Malik, "Analysis and design of fractal antenna for efficient communication network in vehicular model," *Sustainable Computing: Informatics and Systems*, Elsevier, Jun. 2021.

28. Madhav, B. T. P. and T. Anilkumar, "Design and study of multiband planar wheel-like fractal antenna for vehicular communication applications," *Microwave & Optical Technology Letters*, Wiley, 2017.

29. Weng, L. H., Y. C. Guo, X. W. Shi, and X. Q. Chen, "An overview on defected ground structure," *Progress In Electromagnetics Research B*, Vol. 7, 173–189, 2008.

30. Wang, L., J. Yu, T. Xie, and K. Bi, "A novel multiband fractal antenna for wireless application," *International Journal of Antennas and Propagation*, Vol. 2021, Article ID 9926753, 9 pages, 2021.

31. Gurjar, R., D. K. Upadhyay, B. K. Kanaujia, and A. Kumar, "A compact modified sierpinski carpet fractal UWB MIMO antenna with square shaped funnel-like ground stub," *AEU — Int. J. Electron. Commun.*, Vol. 117, 153126, 2020, ISSN 1434-8411.

32. Sabir, M. and G. Ratnu, "A design of compact T-shaped fractal patch antenna for X-band applications," *Mater. Today Proc.*, Vol. 29, Part 2, 295–299, 2020, ISSN 2214-7853.

33. Singh, J., R. Stephan, and M. A. Hein, "Low profile Penta band automotive patch antenna using horizontal stacking and corner feeding," *IEEE Access*, Vol. 7, 74198–74205, May 2019.

34. Madhav, B. T. P. and T. Anilkumar, "Design and study of multiband planar wheel-like fractal antenna for vehicular communication applications," *Microwave & Optical Technology Letters*, Wiley, 2017.

35. Cheng, Y., J. Lu, and C. Wang, "Design of a multiple band vehicle-mounted antenna," *Hindawi International Journal of Antennas and Propagation*, Vol. 2019, Article ID 6098014, 2019.

36. Agrawal, N., A. K. Gautam, and K. Rambabu, "Design and packaging of multi-polarized triple-band antenna for automotive applications," *International Journal of Electronics and Communications*, Vol. 113, Jan. 2020.

37. Wang, L., J. Yu, T. Xie, and K. Bi, "A novel multiband fractal antenna for wireless application," *International Journal of Antennas and Propagation*, Vol. 2021, Article ID 9926753, 9 pages, 2021.